The magnetic moment operator reproducing these matrix elements in the selected four-dimensional $J = 0, 1$ subspace can be written down in an elegant way

$$\boldsymbol{M} = 2\boldsymbol{S} - \boldsymbol{L}^{\text{eff}} = -\sqrt{6}\, i(s^\dagger \boldsymbol{T} - \boldsymbol{T}^\dagger s) - \tfrac{1}{2}\, i(\boldsymbol{T}^\dagger \times \boldsymbol{T})\,. \tag{2.90}$$

In this form it is clear that the major potential to generate a magnetic moment have the transitions between s and $\boldsymbol{T}$ states, the second part is the already mentioned contribution of the $\boldsymbol{J}$ moment of the triplet that is equivalent to $-i(\boldsymbol{T}^\dagger \times \boldsymbol{T})$ within the $J = 0, 1$ subspace.

2.3 Electronic hopping and tight-binding approximation

So far we have been dealing with the (rather complex) physics of correlated valence shells of the individual ions. In this section we are going to activate connections between the ions in the form of electronic hopping. There will not be any many-body aspects discussed here as our main goal is just to get the matrix elements enabling a single electron to move from site to site – so-called tight-binding parameters entering a single-electron hopping Hamiltonian. As a motivating example we start by considering independent electrons moving in a crystal consisting of identical atoms arranged in a simple lattice. Their wavefunctions obey the Schrödinger equation

$$\left[-\frac{\hbar^2}{2m}\nabla^2 + \sum_{\boldsymbol{R}} V_{\text{at}}(\boldsymbol{r} - \boldsymbol{R})\right] \Psi = E\Psi\,, \tag{2.91}$$

where $V_{\text{at}}(\boldsymbol{r} - \boldsymbol{R})$ is the atomic potential for an atom placed at site $\boldsymbol{R}$. Summed through the lattices sites, the atomic potentials generate a periodic crystal potential. In the tight-binding approximation to the problem (2.91), one assumes that the relevant states are well localized so that the electron wavefunctions can be constructed as linear combinations of atomic orbitals. This concept is illustrated by Fig. 16 where we construct a virtual two-dimensional crystal made out of potential wells of circular symmetry and study the evolution of its energy levels when reducing the lattice spacing, i.e. bringing the initially isolated atoms closer to each other. At very large lattice spacing, the spectrum of energy levels has a discrete structure below the top of the crystal potential, corresponding to the individual bound states of the isolated wells. Above that threshold energy, delocalized states forming a continuum are found. As we bring the "atoms" closer and closer, the localized states start to overlap and their interaction produces energy bands of increasing bandwidth. The higher-energy bound states are forming bands sooner because they have a larger spatial extent and overlap more easily. This is an analogy of the atomic orbitals in a crystal - the valence ones form bands while the deep electron levels retain their atomic character. It is intuitively clear that in the situation with rather well localized states (the electrons are "tightly bound" to their atoms), the appropriate model Hamiltonian should be of the form

$$\mathcal{H}_{\text{TB}} = \sum_{n\boldsymbol{R}} \left[\varepsilon_n\, c^\dagger_{n\boldsymbol{R}} c_{n\boldsymbol{R}} - \sum_{n'\Delta\boldsymbol{R}} t_{nn'}(\Delta\boldsymbol{R})\, c^\dagger_{n',\boldsymbol{R}+\Delta\boldsymbol{R}}\, c_{n\boldsymbol{R}}\right]\,, \tag{2.92}$$

where the operators $c^\dagger_{n\boldsymbol{R}}$ and $c_{n\boldsymbol{R}}$ create/annihilate an electron in the state $|\phi_{n\boldsymbol{R}}\rangle$ corresponding to orbital n at site $\boldsymbol{R}$. The first part of this tight-binding Hamiltonian $\mathcal{H}_{\text{TB}}$ just counts the energies of the occupied orbitals [c.f. the energies ε_α in (2.46)], the second part captures the hopping of electrons between the orbitals located at $\boldsymbol{R}$ and $\boldsymbol{R} + \Delta\boldsymbol{R}$. The amplitudes of the hopping processes are the matrix elements of the original crystal Hamiltonian such as that of Eq. (2.91): $t_{nn'}(\Delta\boldsymbol{R}) = -\langle\phi_{n',\boldsymbol{R}+\Delta\boldsymbol{R}}|\,\mathcal{H}\,|\phi_{n\boldsymbol{R}}\rangle$. The signs are introduced in such a way that the hopping parameters t will be mostly positive. For the sake of brevity, we ignore spin that is

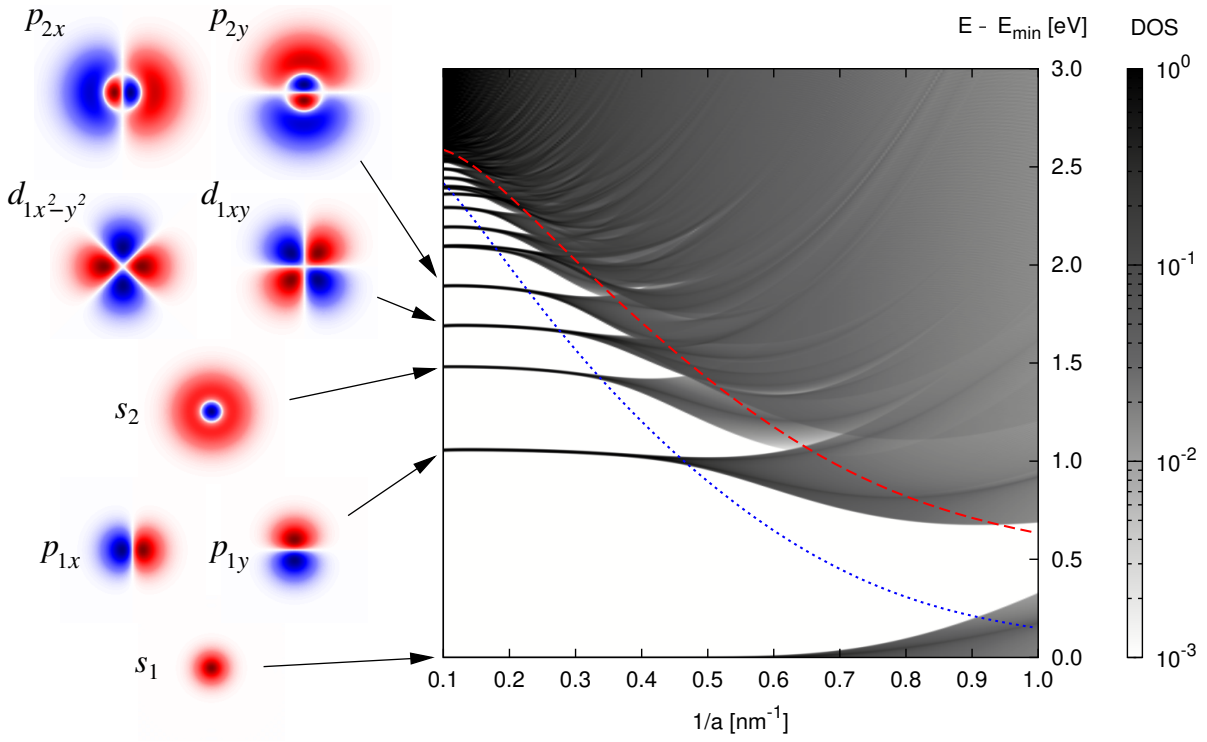

Fig. 16: (left) Wavefunctions of the lowest eigenstates in the potential well described by the 2D potential $V_{\rm at}(r) = V_0 \exp(-\kappa r)\, r_0/(r + r_0)$ with $V_0 = 5$ eV, $\kappa = 0.5$ nm^{-1}, $r_0 = 0.5$ nm. The indicated levels are either non-degenerate or two-fold degenerate and they are labeled in analogy with atomic orbitals. (right) Density of states for a square lattice of the above wells as function of the inverse lattice spacing $1/a$. The energy is measured from the lowest eigenstate. For a large spacing (small $1/a$) the wells are practically isolated and the density of states shows discrete peaks at the energies of bound states. Blue dotted line indicates the average potential level, the red dashed line the top of the potential. The data to construct this figure were obtained by solving Eq. (2.91) by plane-wave expansion method.

conserved during the hopping and would come as an extra index σ together with $\sum_\sigma$. While the values of hopping amplitudes are not known yet, one can expect that the nearest-neighbor and possibly second nearest-neighbor ones will be most important and – in the case of more orbitals involved – also anticipate their symmetry structure [see Fig. 17(a) and (b) for two examples].

Owing to the periodicity of the lattice, the Hamiltonian can be easily diagonalized by employing Bloch waves assembled as linear combinations of the atomic orbitals:

$$|n\boldsymbol{k}\rangle = \frac{1}{\sqrt{N}} \sum_{\boldsymbol{R}} \mathrm{e}^{i\boldsymbol{k}\cdot\boldsymbol{R}}\, |\phi_{n\boldsymbol{R}}\rangle\,. \tag{2.93}$$

Here N denotes the total number of sites in the crystal and normalizes $|n\boldsymbol{k}\rangle$ to unity when the overlaps of orbitals at different sites are negligible. By inserting the consistently transformed electron operators $c_{n\boldsymbol{R}} = N^{-1/2} \sum_{\boldsymbol{k}} \mathrm{e}^{i\boldsymbol{k}\cdot\boldsymbol{R}} c_{n\boldsymbol{k}}$ into $\mathcal{H}_{\rm TB}$, it acquires the form with separated contributions of the individual Bloch vectors $\boldsymbol{k}$

$$\mathcal{H}_{\rm TB} = \sum_{\boldsymbol{k}} \sum_{nn'} \left[\varepsilon_n \delta_{nn'} - \sum_{\Delta\boldsymbol{R}} t_{nn'}(\Delta\boldsymbol{R})\, \mathrm{e}^{-i\boldsymbol{k}\cdot\Delta\boldsymbol{R}} \right] c^\dagger_{n'\boldsymbol{k}} c_{n\boldsymbol{k}}\,. \tag{2.94}$$

For each $\boldsymbol{k}$, it remains to diagonalize a matrix whose dimension is equal to the number of orbitals involved (no diagonalization is thus needed in case of one relevant orbital). For the two examples

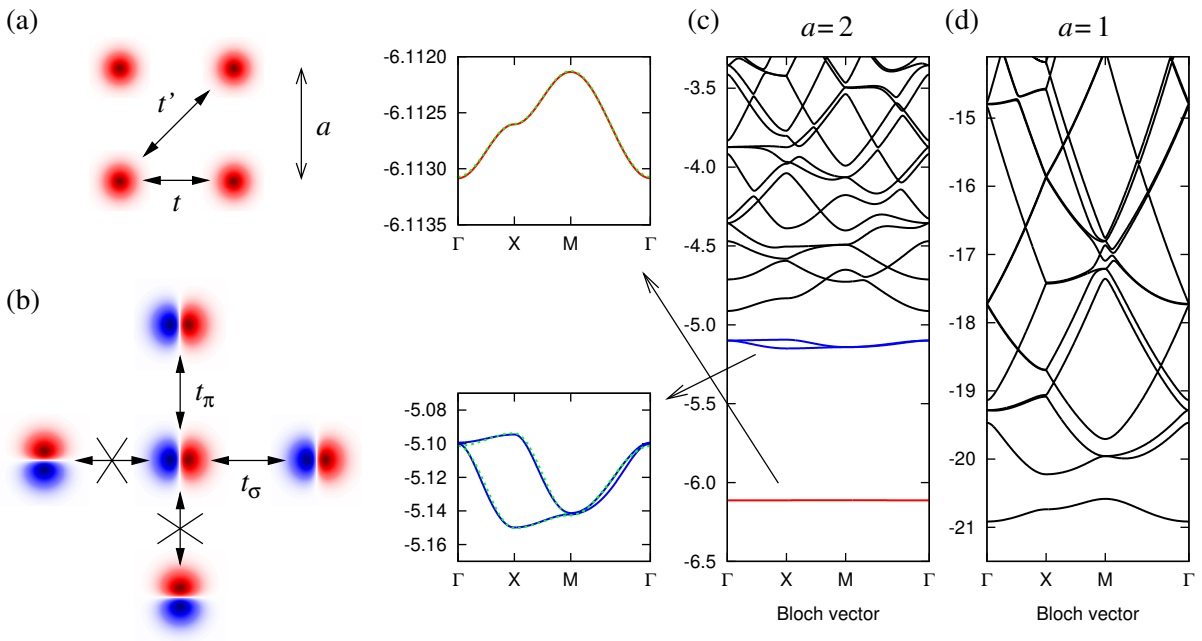

Fig. 17: (a) Hopping processes included in the simplest tight-binding approximation for the bands derived from s "orbitals" of Fig. 16 in a square lattice. Nearest-neighbor and next nearest-neighbor hopping amplitudes t and t' are indicated. (b) Hopping processes involving the p orbitals on a square lattice. The symmetry of these states makes certain hopping amplitudes to vanish, the non-zero ones depend on the relative orientation of the orbitals (t_σ and t_π). (c) Band structure obtained for the setup of Fig. 16 and the value $a = 2\,\mathrm{nm}$ of the lattice parameter. The weakly dispersing bands derived from the s_1 and p_1 levels are shown in detail on the left. The green dashed lines are fits by the corresponding nearest-neighbor tight-binding dispersion relations. The band structure is plotted along the conventional path involving $\Gamma = (0,0)$, $\mathrm{X} = (\pi/a, 0)$ and $\mathrm{M} = (\pi/a, \pi/a)$ points in the Brillouin zone. (d) Band structure for $a = 1\,\mathrm{nm}$ where even the lowest level already shows a significant dispersion. Its profile seems to be just a scaled version of that from panel (c), demonstrating the applicability of the tight-binding scheme.

in Fig. 17(a),(b) we get

$$\mathcal{H}_{\mathrm{TB}} = \sum_{\boldsymbol{k}} \left[\varepsilon_s - 2t(\cos k_x a + \cos k_y a) - 4t' \cos k_x a \cos k_y a\right] c^\dagger_{\boldsymbol{k}} c_{\boldsymbol{k}} \tag{2.95}$$

and

$$\mathcal{H}_{\mathrm{TB}} = \sum_{\boldsymbol{k}} \begin{pmatrix} c^\dagger_{p_x \boldsymbol{k}} & c^\dagger_{p_y \boldsymbol{k}} \end{pmatrix} \begin{pmatrix} \varepsilon_p - 2t_\sigma \cos k_x a - 2t_\pi \cos k_y a & 0 \\ 0 & \varepsilon_p - 2t_\pi \cos k_x a - 2t_\sigma \cos k_y a \end{pmatrix} \begin{pmatrix} c_{p_x \boldsymbol{k}} \\ c_{p_y \boldsymbol{k}} \end{pmatrix} \tag{2.96}$$

giving directly the dispersion relations of electrons. In the latter case, nonzero off-diagonal elements would be generated by next nearest-neighbor hopping, nearest-neighbor pairs of p_x and p_y orbitals are not connected due to symmetry reasons. The band structures obtained numerically by solving the full problem (2.91) are presented in Fig. 17 and contrasted to those resulting in nearest-neighbor tight-binding approximation. A remarkable agreement is obtained when choosing the proper values of the few parameters (ε_s and t or ε_p and t_σ, t_π), in particular for the s band derived from the most localized bound state.

As we have just seen, the tight-binding approximation is a useful tool well capturing the dispersion of the bands derived from localized states. Its success relies on a limited range of